

# Mathematical Simulation of Propane Dehydrogenation Involving Oxygen on an Alumina–Chromium Catalyst Promoted with Co, Ni, Bi, and K Oxides

R. P. Dzhafarov, S. M. Gadzhizade, S. A. Dzhamalova, N. A. Aliev, and A. A. Kasimov

Mamedaliev Institute of Petrochemical Processes, Academy of Sciences of Azerbaijan, Baku, 370025 Azerbaijan

e-mail: djafarov\_rasim@mail.ru

Received June 21, 2011

**Abstract**—The rate laws of propane dehydrogenation involving oxygen on an alumina–chromium catalyst promoted with Co, Ni, Bi, and K oxides were studied. The reaction was carried out in a flow reactor in the temperature range of 560–640°C at residence times of 0.5–2.5 s. A kinetic model of the process according to a probable reaction scheme was proposed. The rate constants and activation energies of individual reactions that participate in the process were found. A mathematical model of the process was developed with consideration for material and heat balances and hydrodynamic conditions. The concentration and temperature fields and pressure along the height of the catalyst bed were calculated. The dependences of the target product yield and process selectivity on the residence time were plotted.

**DOI:** 10.1134/S002315841202005X

## INTRODUCTION

An increase in the production of synthetic rubber requires use of a significant quantity of monomers obtained from the pyrolytic fraction. However, the development of the pyrolysis technology lags behind the steady increase in the production of synthetic rubber, and this gives an additional impetus to in-depth research of the dehydrogenation of C<sub>3</sub>–C<sub>4</sub> paraffins into the corresponding olefins.

Olefins (propylene, *n*-butenes, and isobutylene) find wide application in the production of synthetic rubbers, plastics, components of motor gasoline, and other valuable chemical products. This is the reason why interest in the intensification of methods for their production has not weakened over half a century all over the world. Most of the existing intensification methods pertain to the catalytic dehydrogenation of *n*-paraffins. Because of this, the number of studies on the improvement and development of new catalysts for dehydrogenation increases continuously.

In particular, attention has been focused on the oxidative dehydrogenation of hydrocarbons, which can be performed in the continuous mode to give a high yield of the target product [1–6].

Ramos et al. [7] considered the kinetics of the oxidative dehydrogenation of propane into propylene on a V/MgO catalyst. They assumed that one of the two active sites of the catalyst selectively converts propane into propylene, and the other oxidizes propylene to CO<sub>2</sub>. The kinetic parameters were evaluated for the reaction conducted in an integral reactor and in an inert membrane reactor. Chem et al. [8] studied the

kinetics and mechanism of the oxidative dehydrogenation of propane on vanadium, molybdenum, and tungsten oxides. The oxidative dehydrogenation of propane was also studied with the use of vanadium catalysts based on Al<sub>2</sub>O<sub>3</sub>, TiO<sub>2</sub>, ZrO<sub>2</sub>, and MgO [9] and other catalysts [10–12]. There have been reports on the kinetics of the oxidative dehydrogenation of C<sub>4</sub> paraffins on different catalysts [13–17].

Here, we report the kinetics of propane dehydrogenation involving oxygen on a highly active alumina–chromium catalyst and a mathematical model taking into account the material and heat balances and hydrodynamic conditions.

## EXPERIMENTAL

The rate laws of propane dehydrogenation involving oxygen were studied in a laboratory flow-type reactor with a fixed bed of a catalyst in the temperature range of 833–913 K at a gas mixture (propane, oxygen, and nitrogen) space velocity of 1440–7200 h<sup>−1</sup> and a molar ratio of 0.1 : 1 : 15 between oxygen, propane, and nitrogen. The reaction was performed under isothermal conditions. The reactor temperature was controlled with a thermocouple. The initial hydrocarbon and also oxygen and nitrogen were supplied with the use of a graduated flow meter.

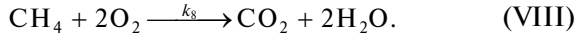
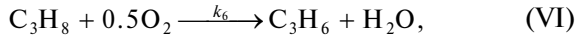
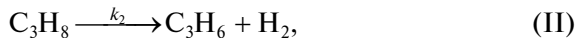
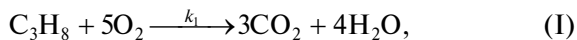
The reaction was monitored by analyzing samples of the reaction mixture on an LKhM-80 chromatograph. Sampling was started 30 min after the beginning of the reaction, when the system had reached a steady state of continuous propane conversion. The catalyst retained its activity for more than 30 days.

Powdered  $\text{Al}_2\text{O}_3$  with a particle diameter of 0.063 mm was used as the support. To obtain the respective oxides, Cr, Ni, Co, Bi, and K nitrates were preliminarily calcined and then mixed with  $\gamma\text{-Al}_2\text{O}_3$ . Distilled water was added to the mixture obtained by dry mixing, and the contents were continuously stirred for 2 days; thereafter, water was evaporated at 30–50°C to obtain a paste-like substance. Next, the catalyst was pelletized, dried under reduced pressure at 100–120°C, and calcined under the same conditions at 640–650°C. The residual pressure was 10–15 Torr. The catalyst prepared under the reduced pressure contained 10–15% Cr, 2.5–4% Ni, 2–3% Co, 3–5% Bi, 1–3% K, and the balance  $\gamma\text{-Al}_2\text{O}_3$ . The preparation of the catalyst under the reduced pressure led to the formation of pores with a narrow size distribution, which facilitated enhancement of its activity and selectivity. In this case, the specific surface area of the catalyst increased from 60 to 125  $\text{m}^2/\text{g}$  and the specific volume increased from 0.16 to 0.18  $\text{m}^3/\text{g}$ .

## RESULTS

To reveal the main laws governing the process and thereby deduce its probable mechanism, we studied the effect of reaction conditions on the formation of the products. The presence of  $\text{CO}_2$  among the reaction products is evidence of the deep oxidation of propane and propylene. The analysis of contact gas showed that oxygen-containing compounds other than  $\text{CO}_2$  (aldehydes, ketones, and acids) were absent from the products. This fact allowed us to ignore the successive conversions of propylene. CO was not detected in the contact gas either.

Table 1 summarizes the results of kinetic experiments [18]. The yield of the target product propylene at 893 K was 60–63 mol %, and the process selectivity was 90–91 mol %. The rate laws that we found allowed us to propose a probable mechanism, from which we derived the following chemical equations to describe the individual reactions involved in the process:



According to the law of mass action, the kinetic model can be described by the following system of differential equations:

$$\frac{dC_1}{d\tau} = -(k_1 C_7^{n_2} + k_2 + k_3 + k_6 C_7^{n_2}) C_1^{n_1}, \quad (1)$$

$$\frac{dC_2}{d\tau} = (k_2 + k_6 C_7^{n_2}) C_1^{n_1} - \left( k_4 C_7^{n_2} + \frac{2}{3} k_5 \right) C_2^{n_3}, \quad (2)$$

$$\frac{dC_3}{d\tau} = \left( \frac{1}{3} k_1 C_1^{n_1} + \frac{1}{3} k_4 C_2^{n_3} + \frac{1}{2} k_7 C_5^{n_4} + k_8 C_6^{n_5} \right) C_7^{n_2}, \quad (3)$$

$$\begin{aligned} \frac{dC_4}{d\tau} = & \left( \frac{1}{4} k_1 C_1^{n_1} + \frac{1}{3} k_4 C_2^{n_3} \right. \\ & \left. + k_6 C_1^{n_1} + \frac{1}{2} k_7 C_5^{n_4} + \frac{1}{2} k_8 C_6^{n_5} \right) C_7^{n_2}, \end{aligned} \quad (4)$$

$$\frac{dC_5}{d\tau} = k_3 C_1^{n_1} + \frac{3}{2} k_5 C_2^{n_3} - k_7 C_5^{n_4} C_7^{n_2}, \quad (5)$$

$$\frac{dC_6}{d\tau} = k_3 C_1^{n_1} - k_8 C_6^{n_5} C_7^{n_2}, \quad (6)$$

$$\begin{aligned} \frac{dC_7}{d\tau} = & - \left( 5k_1 C_1^{n_1} + 4 \frac{1}{2} k_4 C_2^{n_3} \right. \\ & \left. + \frac{1}{2} k_6 C_1^{n_1} + 3k_7 C_5^{n_4} + 2k_8 C_6^{n_5} \right) C_7^{n_2}, \end{aligned} \quad (7)$$

$$\frac{dC_8}{d\tau} = k_2 C_1^{n_1}, \quad (8)$$

where  $C_1, C_2, C_3, C_4, C_5, C_6, C_7$ , and  $C_8$  are the concentrations of propane, propylene,  $\text{CO}_2$ , water, ethylene, methane, oxygen, and hydrogen, respectively;  $k_1, k_2, k_3, k_4, k_5, k_6, k_7$ , and  $k_8$  are the rate constants of particular reactions;  $n_1, n_2, n_3, n_4$ , and  $n_5$  are the orders of the reaction with respect to particular components; and  $\tau$  is the residence time.

The problem was reduced to determination of the rate constants  $k_i$  and orders  $n_i$  in the system of differential equations (1)–(8). The kinetic constants were calculated with the use of the algorithm for searching a minimum of a function of many variables involving the modified Runge–Kutta method for solving high order differential equations [19]. The search was continued until the difference between the experimental and computed values reached a minimum. Table 2 summarizes the results of calculating the rate constants. The orders  $n_i$  are close to 1. Assuming that the temperature dependence of the reaction rate constants obeys the Arrhenius law [20], we also calculated the activation energies  $E_a$  and the preexponential factors  $k_0$  (Table 2).

The kinetic model based on the chosen mechanism and the corresponding rate constants adequately describes the process. The maximum deviation of the calculated concentrations from the experimental values do not exceed 7%. Thus, the data calculated using the model are in satisfactory agreement with the results of the kinetic experiment.

**Table 1.** Experimental concentrations of the initial components and reaction mixture products during propane dehydrogenation involving oxygen

Temper- ature, K	Residence time, s	Concentration $C_i \times 10^4$ , mol/L						
		$C_3H_8$	$C_3H_6$	$CO_2$	$H_2O$	$C_2H_4$	$CH_4$	$O_2$
833	0.0	8.89	0	—	—	—	0	0.893
	0.5	8.08	0.74	0.006	0.00438	0.012	0.0104	0.845
	1.0	7.36	1.408	0.05	0.095	0.0254	0.0205	0.72
	1.5	6.69	2.02	0.118	0.291	0.0428	0.0293	0.57
	2.0	6.05	2.58	0.196	0.568	0.0646	0.0374	0.386
	2.5	5.49	3.09	0.266	0.831	0.0917	0.0454	0.094
853	0.0	8.68	0	0	0	0	0	0.87
	0.5	7.67	0.854	0.0098	0.0068	0.0244	0.0186	0.778
	1.0	6.77	1.62	0.089	0.137	0.0472	0.0352	0.61
	1.5	5.97	2.31	0.202	0.41	0.0687	0.05	0.395
	2.0	5.25	2.96	0.31	0.714	0.089	0.0636	0.181
	2.5	4.62	3.46	0.37	0.941	0.31	0.175	0.0034
873	0.0	8.48	0	0	0	0	0	0.85
	0.5	6.73	1.245	0.013	0.0096	0.053	0.0182	0.716
	1.0	5.32	2.258	0.0182	0.254	0.097	0.044	0.475
	1.5	4.18	3.98	0.122	0.601	0.274	0.08	0.225
	2.0	3.27	4.73	0.335	0.76	0.433	0.209	0.0014
	2.5	2.54	5.27	0.435	0.866	0.861	0.432	0.0002
893	0.0	8.29	0	0	0	0	0	0.83
	0.5	6.24	1.31	0.0125	0.00897	0.107	0.0438	0.704
	1.0	4.63	2.34	0.144	0.326	0.192	0.078	0.435
	1.5	3.4	4.15	0.283	0.761	0.251	0.105	0.156
	2.0	2.45	4.96	0.349	0.996	0.483	0.325	0.00015
	2.5	1.93	4.72	0.445	1.05	0.79	0.44	0.0000
913	0.0	8.1	0	0	0	0	0	0.81
	0.5	4.78	1.66	0.022	0.0172	0.288	0.25	0.52
	1.0	2.84	2.64	0.273	0.364	0.463	0.41	0.27
	1.5	1.69	3.22	0.458	0.622	0.562	0.5	0.094
	2.0	1.01	4.57	0.514	0.7	0.91	1.04	0.0022
	2.5	0.61	4.17	0.52	0.707	1.65	1.47	—

The kinetic model of propane dehydrogenation involving oxygen can be accepted as the basis for designing a pilot adiabatic reactor.

### SIMULATION AND OPTIMIZATION OF THE PROCESS IN AN ADIABATIC REACTOR

In the mathematical description of the fixed bed of the catalyst, we used a quasi-homogeneous model of a granular catalyst bed. According to this model, the catalyst bed is represented as a permeable continuous medium through which a gas flows and a chemical reaction occurs at a rate equal to the observed rate of

conversion. In this case, the catalyst bed is considered as a homogeneous medium with continuous distributions of concentration, temperature, pressure, and flow rate. The reaction rates are averaged over the bed volume, and heat and mass transfer is characterized in terms of effective thermal conductivity and diffusion coefficients, which depend on the physical properties of the mixture, on the flow rate, on the sizes and shapes of the grains, and on the structure of the granular bed.

There is no heat and mass transfer in the adiabatic catalyst bed. Heat transfer within grains occurs mainly through the solid catalyst, whose bulk thermal con-

**Table 2.** Kinetic parameters of propane dehydrogenation involving oxygen

Constant	Temperature, K					$E_a$ , kcal/mol	$k_0$
	833	853	873	893	913		
$k_1, \text{L mol}^{-1} \text{s}^{-1}$	$0.14 \times 10^{-3}$	$0.28 \times 10^{-3}$	$0.57 \times 10^{-3}$	$1.1 \times 10^{-3}$	$2.1 \times 10^{-3}$	51.35	$0.41 \times 10^{10}$
$k_2, \text{s}^{-1}$	0.16	0.22	0.31	0.42	0.55	23.38	$0.22 \times 10^6$
$k_3, \text{s}^{-1}$	$0.35 \times 10^{-2}$	$0.79 \times 10^{-2}$	$1.72 \times 10^{-2}$	$3.63 \times 10^{-2}$	$7.4 \times 10^{-2}$	57.65	$0.46 \times 10^{13}$
$k_4, \text{L mol}^{-1} \text{s}^{-1}$	$0.84 \times 10^{-2}$	$1.23 \times 10^{-2}$	$1.76 \times 10^{-2}$	$2.48 \times 10^{-2}$	$3.45 \times 10^{-2}$	26.70	$0.85 \times 10^5$
$k_5, \text{s}^{-1}$	$0.46 \times 10^{-4}$	$0.85 \times 10^{-4}$	$1.52 \times 10^{-4}$	$2.65 \times 10^{-4}$	$4.5 \times 10^{-4}$	42.98	$0.87 \times 10^7$
$k_6, \text{L mol}^{-1} \text{s}^{-1}$	$0.35 \times 10^{-3}$	$0.55 \times 10^{-3}$	$0.85 \times 10^{-3}$	$1.29 \times 10^{-3}$	$1.92 \times 10^{-3}$	32.02	$0.88 \times 10^5$
$k_7, \text{L mol}^{-1} \text{s}^{-1}$	$0.1 \times 10^{-3}$	$0.155 \times 10^{-3}$	$0.24 \times 10^{-3}$	$0.35 \times 10^{-3}$	$0.52 \times 10^{-3}$	31.18	$0.15 \times 10^5$
$k_8, \text{L mol}^{-1} \text{s}^{-1}$	1.57	1.88	2.23	2.63	3.1	12.52	$0.3 \times 10^4$

**Table 3.** Heat capacities and the heats of combustion of mixture components and heats of reactions

Mixture component	$C_p, \text{cal mol}^{-1} \text{K}^{-1}$	Heat of combustion $\Delta H, \text{cal/mol}$	Heat of reaction, cal/mol
$\text{C}_3\text{H}_8$	33.91	18250	118 ( $\Delta H_1$ )
$\text{C}_3\text{H}_6$	28.71	15244	1338 ( $\Delta H_2$ )
$\text{CO}_2$	10.85	6811	-507 ( $\Delta H_3$ )
$\text{H}_2\text{O}$	9.51	5380	103 ( $\Delta H_4$ )
$\text{C}_2\text{H}_4$	18.54	10152	-32 ( $\Delta H_5$ )
$\text{C}_2\text{H}_4$	17.28	7591	15.5 ( $\Delta H_6$ )
$\text{O}_2$	7.53	4717	79 ( $\Delta H_7$ )
$\text{H}_2$	7.31	4344	546 ( $\Delta H_8$ )

ductivity is higher than the thermal conductivity of the gas by several orders of magnitude.

The influence of axial diffusion is insignificant because industrial catalyst beds are fairly long. Heat and mass transfer is due to turbulent diffusion at Reynolds numbers larger than 100. Under these conditions, molecular diffusion can be ignored and the hydrodynamic regime is similar to plug flow [21]. It was experimentally established that propane dehydrogenation involving oxygen is kinetically controlled. The internal-diffusion effect can be ignored because a change in the catalyst granule size from 0.8 to 3 mm does not exert a considerable effect on the yield of the target product. For this reason, the plug flow model was accepted for the adiabatic reactor.

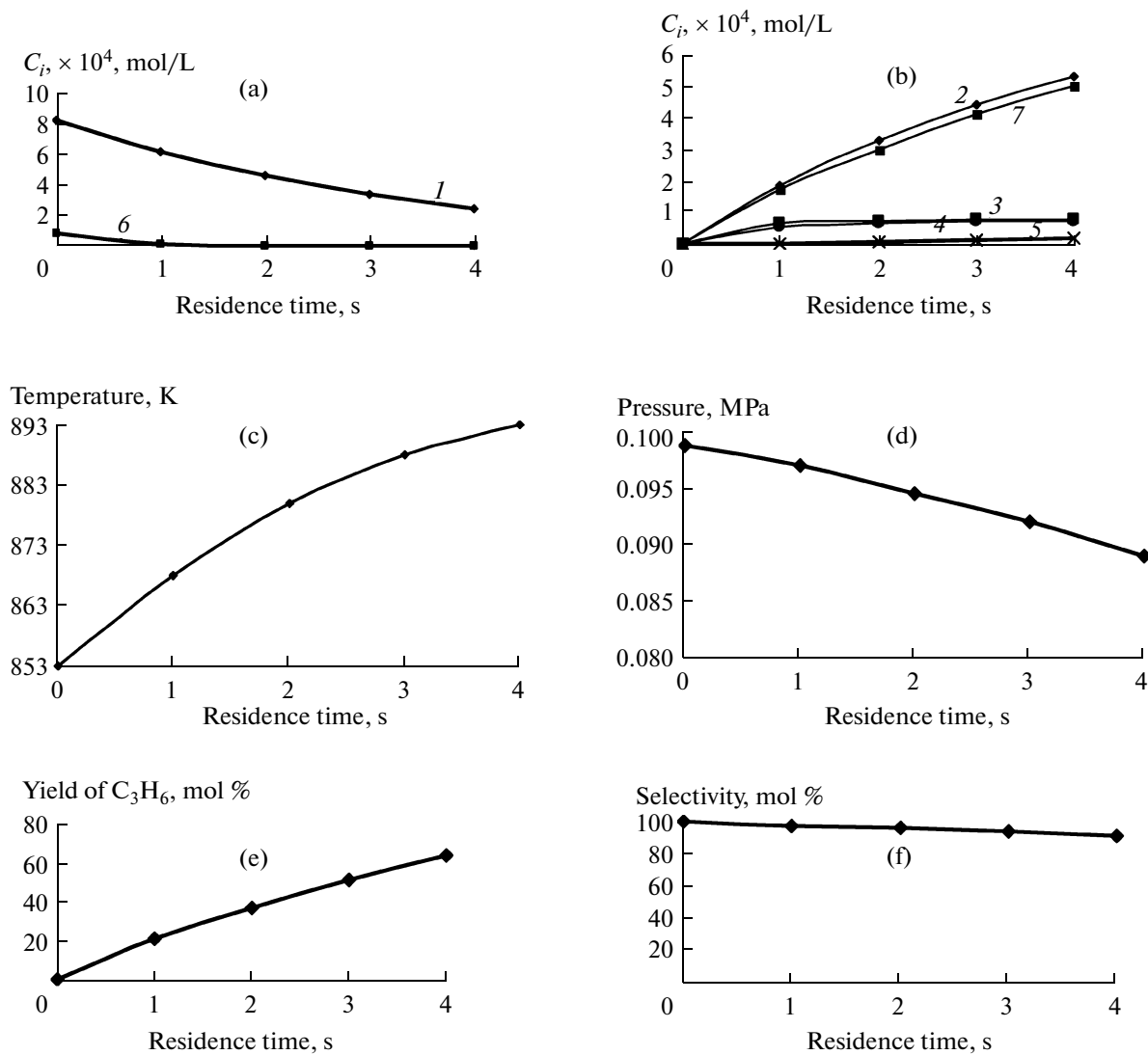
For mathematical description of the reactor, kinetic model (1)–(8) should be supplemented with the following heat balance and hydrodynamic equations:

$$\frac{dT}{d\tau} = -\frac{1}{C_p(T)} \sum \Delta H_i \frac{dC_i}{d\tau}, \quad (9)$$

$$\frac{dP}{d\tau} = -\left(\frac{150}{\text{Re}} + 1.75\right) \frac{\rho_{\text{gas}} U_0^2 (1-\varepsilon)}{d_p g \varepsilon^3} 0.987 \times 10^{-5}. \quad (10)$$

Here,  $\text{Re}$  is the Reynolds number  $\frac{d_p \rho_{\text{gas}} U_0}{\mu(1-\varepsilon)}$ ,  $\rho_{\text{gas}}$  is the density of the gas ( $\text{kg/m}^3$ ),  $g$  is the acceleration of gravity ( $\text{m/s}^2$ ),  $U_0$  is the linear velocity of the gas ( $\text{m/s}$ ),  $d_p$  is the equivalent diameter of particles ( $\text{m}$ ),  $\varepsilon$  is the bed voidage (dimensionless quantity),  $\mu$  is the viscosity of the gas ( $\text{kg m}^{-1} \text{s}^{-1}$ ),  $\Delta H_i$  is the heat of the  $i$ th reaction (cal/mol),  $C_p$  is the average heat capacity of the reactants ( $\text{cal mol}^{-1} \text{K}^{-1}$ ),  $T$  is the gas mixture temperature (K), and  $C_i$  is the concentration of the  $i$ th component (mol/L).

Table 3 summarizes the heat capacities and the heats of combustion of individual mixture components (reference data [22–24]). The heats of individual reactions were calculated according to the Hess law, subtracting the sum of the heats of combustion of the resulting reaction products from the sum of the heats of combustion of the initial substances.



Dependence of the reaction parameters of the oxidative dehydrogenation of propane in an adiabatic reactor on the residence time: (a) concentrations of the initial substances (1,  $\text{C}_3\text{H}_8$ ; 6,  $\text{O}_2$ ), (b) concentrations of the reaction products (2,  $\text{C}_3\text{H}_6$ ; 3,  $\text{CO}_2$ ; 4,  $\text{H}_2\text{O}$ ; 5,  $\text{C}_2\text{H}_4 + \text{CH}_4$ ; and 7,  $\text{H}_2$ ), (c) temperature, (d) pressure, (e) yield of the target product, and (f) process selectivity.

For simulation of the adiabatic reactor, the following conditions were selected: fixed catalyst bed 1.2 m in length; catalyst particle diameter  $d_p = 3 \times 10^{-3}$  m; linear gas mixture velocity of  $U_0 = 0.3$  m/s; gas density of  $\rho_{\text{gas}} = 1.63$  kg/m<sup>3</sup>; dynamic viscosity of  $\mu = 3.97 \times 10^{-6}$  kg m<sup>-1</sup> s<sup>-1</sup>; catalyst bed density of  $\rho_{\text{bed}} = 960$  kg/m<sup>3</sup>; apparent particle density of  $\rho_a = 1600$  kg/m<sup>3</sup>. The voidage of the catalyst bed was determined via the equation  $\varepsilon = \rho_a - \rho_{\text{bed}}/\rho_a$ . Knowing the numerical values of  $\rho_{\text{gas}}$ ,  $\mu$ ,  $\varepsilon$ ,  $d_p$ , and  $U_0$ , we determined the Reynolds number:

$$\text{Re} = \frac{\rho_{\text{gas}} U_0 d_p}{\mu(1 - \varepsilon)} = \frac{1.63 \cdot 0.3 \cdot 3 \times 10^{-3}}{3.97 \times 10^{-6} \cdot 0.6} = 616.$$

Because the value of Re falls within the range  $100 < \text{Re} \leq 4000$  [25], we used the equation  $f_p = \frac{150}{\text{Re}} + 1.75$  to find the drag coefficient  $f_p = \frac{150}{616} + 1.75 = 1.993$ . Then, from Eq. (10), it follows that  $-\frac{dP}{d\tau} = \frac{1.993 \cdot 0.3 \cdot 0.6 \cdot 1.63}{3 \times 10^{-3} \cdot 0.4^3} = 3.0455 \times 10^3 \text{ N m}^{-2} \text{ s}^{-1}$ .

Substituting the optimum process parameters  $V = 60 \text{ h}^{-1}$  and  $\text{O}_2 : \text{C}_3\text{H}_8 : \text{N}_2 = 0.1 : 1 : 15$  into the complete mathematical model, we obtain the distributions of the concentrations of the initial substances and reaction products, the gas mixture temperature, and the pressure along the reactor and also data on the yield of the target product and the process selectivity (figure). As can be seen in the figure, at a residence

time of 4 s, the gas temperature in the adiabatic reactor increases from 853 to 893 K and the pressure falls from 0.0987 to 0.089 MPa; that is, the pressure drop is 0.0097 MPa. The propylene yield is 63 mol % on a passed propane basis, and the selectivity (propylene yield on a converted propane basis) is 91 mol %.

## REFERENCES

1. Michorczyk, P. and Qgonowski, J., *Appl. Catal., A*, 2003, vol. 251, p. 425.
2. Bhasin, M.M., McGain, J.H., Vora, B.V., Imai, T., and Pujado, P.R., *Appl. Catal., A*, 2001, vol. 221, p. 379.
3. Agaskor, P.A., Grasselli, R.K., Michaels, P.T., Reischman, P.T., Stem, D.L., and Tsikoyiamis, J.G., US Patent 5.430.209, 1995.
4. Jibril, B.Y. and Al-Zahrani, S.M., Abasaeed A.E., Hughes R, *Catal. Lett.*, 2003, vol. 87, nos. 3–4, p. 121.
5. Abello, M.C., Gomez, M.F., Casella, M., Feretti, O.A., Bunares, M.A., and Fierro, J.L.G., *Appl. Catal., A*, 2003, vol. 251, no. 2, p. 435.
6. Florenzia, C.C., Manuel, F.G., Luis, A.H., Osmar, H.F., and Morig, C.A., *React. Kinet. Catal. Lett.*, 2004, vol. 81, no. 2, p. 259.
7. Ramos, R., Pilar, P., Menender, M., Santamaria, J., and Patience, S., *Can. J. Chem. Eng.*, 2001, vol. 79, no. 6, p. 902.
8. Chem, K., Bell, A.T., and Iglesia, E., *J. Phys. Chem. B*, 2000, vol. 104, p. 1292.
9. Lemonidou, A.A., Nalbandian, L., and Vasalos, I.A., *Catal. Today*, 2000, vol. 61, p. 333.
10. Lars, S. and Anderson, T., *Appl. Catal., A*, 1994, vol. 112, no. 2, p. 209.
11. Levitsky, A.A., Polyak, S.S., and Shtern, V.Ya., *Int. J. Chem. Kinet.*, 1984, vol. 16, no. 10, p. 1269.
12. Ashmawy, F.M., *J. Chem. Technol. Biotechnol.*, 1984, vol. 34A, p. 183.
13. Agafonov, Yu.A., Nekrasov, N.V., Gaidai, N.A., and Lapidus, A.L., *Kinet. Catal.*, 2007, vol. 48, p. 255.
14. Dejoz, A., Lopez, Nieto J.M., Melo, F., and Vazquez, I., *Ind. Eng. Chem. Res.*, 1997, vol. 36, no. 6, p. 2588.
15. Lemonidou, A.A., *Appl. Catal., A*, 2001, vol. 216, no. 2, p. 277.
16. Madeira, L.M., Portela, M.F., Kaddouri, A., Mazzocchia, C., and Anouchinsky, R., *Catal. Today*, 1998, vol. 40, no. 2, p. 229.
17. Zavoianu, R., Dias, C.R., Soares, A.P.V., and Portela, M.F., *Appl. Catal., A*, 2006, vol. 298, p. 40.
18. Gadzhizade, S.M., Dzhamalova, S.A., Aliev, N.A., and Kasimov, A.A., *Russ. J. Appl. Chem.*, 2009, vol. 82, no. 5, p. 880.
19. Abilov, A.G., Velieva, F.M., and Aliev, F.T., *Paket prikladnykh programm: Otsenka kineticheskikh parametrov mnogomarshrutnykh statsionarnykh kataliticheskikh reaktsii* (Estimation of Kinetic Parameters of Multipath Steady-State Catalytic Reactions: Software Package), Moscow: GOSFAP SSSR, 1987, file no. 5088000096.
20. Emmanuel, N.M. and Knorre, D.G., *Kurs khimicheskoi kinetiki* (Chemical Kinetics), Moscow: Vysshaya Shkola, 1984.
21. Slin'ko, M.G., Dil'man, V.V., Markeev, B.M., and Kponberg, A.E., *Khim. Prom-st.*, 1980, no. 11, p. 22.
22. Kazanskaya, A.S. and Skolbo, V.A., *Raschety khimicheskikh ravnovesii* (Chemical Equilibrium Calculations), Moscow: Vysshaya Shkola, 1974.
23. Vvedenskii, A.A., *Termodinamicheskie raschety neftekhimicheskikh protsessov* (Thermodynamic Calculations for Petrochemical Processes), Leningrad: Gostoptekhizdat, 1960.
24. Vukalovich, M.P., Kirilin, V.A., Remizov, S.A., Siletskii, V.S., and Timofeev, V.N., *Termodinamicheskie svoistva gazov* (Thermodynamic Properties of Gases), Moscow: GNTI, 1953.
25. Ergun, S., *Chem. Eng. Prog.*, 1952, vol. 48, p. 227.